Impact of Estimating Position Offsets on the Uncertainties of GNSS Site Velocity Estimates

JGR Solid Earth

RESEARCH ARTICLE
10.1029/2019JB017705

Impact of Estimating Position Offsets on the Uncertainties of GNSS Site Velocity Estimates

Lei Wang[1,2] **and Thomas Herring**[1]

[1]Department of Earth, Atmospheric and Planetary Sciences, Massachusetts Institute of Technology, Cambridge, MA, USA, [2]Now at Department of Civil, Environmental and Geodetic Engineering, The Ohio State University, Columbus, OH, USA

Key Points:
- Impact of estimating position offsets on uncertainties of GNSS site velocity estimates depends on position errors
- The sensitivity decays rapidly with the increase of the temporal correlation of observation noise
- Adding one additional estimated position offset would increase the median velocity standard deviation by 14

Correspondence to:
L. Wang,
wang.1115@osu.edu

Citation:
Wang, L., & Herring, T. (2019). Impact of Estimating Position Offsets on the Uncertainties of GNSS Site Velocity Estimates. *Journal of Geophysical Research: Solid Earth*, *124*, 13,452–13,467. https://doi.org/10.1029/2019JB017705

Received 18 MAR 2019
Accepted 28 SEP 2019
Accepted article online 16 OCT 2019
Published online 28 DEC 2019

Abstract We study the impact of estimating offsets within GNSS position time series on the uncertainties of site velocity estimates. Site velocity uncertainties are estimated by assuming different observational noise types, including white noise, fractal white noise, flicker noise, first-order Gauss-Markov noise, random walk, fractal random walk, and mixture of flicker noise, and white noise. For each noise type, we assess the sensitivity of the velocity uncertainty to offsets numerically by computing the inflation rate of the uncertainty as the number of offset parameters increases. We show that the sensitivity reduces when the noise becomes more temporally correlated. For the mixture of flicker noise plus white noise, which has been concluded as an appropriate noise model for the majority of current GNSS position time series, the rate uncertainty increases by about 11% as the number of offset parameters doubles from 1 to 2 provided that the white noise does not dominate the flicker noise. Based on the analysis of the Plate Boundary Observatory position time series, we find that adding one additional offset parameter would increase the median velocity standard deviation by 14%, consistent with the result of the simulation study. Such increase is much smaller than the conclusion of a 40% by a previous study. Therefore, given the noise characteristics of current GNSS site position estimates, position offsets have limited impact on uncertainties of site velocity estimates. This result implies that improving instrumentation, even though may introduce position offsets, is the best approach for improving reference frame stability.

1. Introduction

Accurate estimation of GNSS site velocities and their uncertainties is essential for many geodetic and geophysical applications, including global/regional reference frame realization, plate tectonic deformation, glacial isostatic adjustment, and crustal loading deformation (Bock and Melgar, 2016; Herring et al., 2016). Typically, the site velocity is estimated by least squares fitting a linear trend to the position time series, in which offsets (i.e., "discontinuity" or "step") commonly exist due to either natural (e.g., earthquakes and environmental changes) or artificial (e.g., equipment changes, changes in processing strategy, and human errors) causes. In a typical GPS position time series, the occurrence frequency of position offsets ranges from 1 per year to 1 per 19 years (Griffiths and Ray, 2016; Williams, 2003a). It has been known that the unmodeled offsets can bias the site velocity estimate (Gazeaux et al., 2013; Williams, 2003a). In order to avoid the otherwise induced bias in the velocity estimate, the parameters representing offsets need to be simultaneously estimated with the velocity parameter in a least squares estimation.

Including offset parameters in site velocity estimation increases the estimated site velocity uncertainty and thus degrades the stability of the global and regional reference frame realizations. However, the occurrence of position offsets is almost certain due to the processes such as earthquakes and site maintenance. In addition, while some offsets in the time series can be identified either from the site maintenance logs or earthquake catalogs, many offsets remain unidentified reflecting missing log entries or other unknown causes. For example, in the second reprocessing by the International GNSS Service (IGS) (Rebischung et al., 2016), the percentages of the offsets due to equipment changes, earthquakes, and unknown causes are 49%, 31%, and 20% of the total 2,090 detected offsets, respectively (Griffiths and Ray, 2016). It is thus possible that the continuous improvement in offset detection methods would further increase the number of detected

offsets in continuous GNSS position time series (Griffiths and Ray, 2016). It is important to understand the impact of the possible addition of offsets during future reprocessings of global and regional reference stations.

The effect of position offsets on estimated site velocity uncertainties depends not only on the offset epochs within the time series but also on the noise type of the site position time series (Williams, 2003b). It has been long recognized that the noise in GPS site position time series is temporally correlated (Langbein and Johnson, 1997; Mao et al., 1999; Santamaría-Gómez et al., 2011; Williams et al., 2004; Zhang et al., 1997) due to various factors such as unmodeled physical processes, orbital errors, atmospheric errors, monument instability, and multipath. Zhang et al. (1997) analyzed 1.6-year time series of daily positions from 10 GPS sites belonging to the Southern California Permanent GPS Geodetic Array and found significant temporal correlations in all the time series, swhich can be described by either a fractal white noise model with the spectral index of about 0.4±0.2 or a white noise plus flicker noise model. Mao et al. (1999) analyzed the position time series of 3-year length from 23 globally distributed GPS stations and concluded that a white noise plus flicker noise model best characterizes all three components of the site coordinates. Williams et al. (2004) examined a total of 954 continuous GPS position time series whose lengths vary from 16 months to 10 years and concluded that the global solutions are best described by a white noise plus flicker noise model, while the regional solutions have power law spectra with highly variable spectral indices. Santamaría-Gómez et al. (2011) analyzed position time series 2.5 to 13 year long from 275 globally distributed stations and found the best noise model is a combination of white noise and flicker noise with mean amplitudes of 2 mm and 6 mm $\mathrm{yr}^{\frac{1}{4}}$, respectively.

Until recently, position time series analysis typically assumed temporally uncorrelated noise, that is, white noise, due to practical difficulties in incorporating certain correlated noise models into the estimation, as well as the significantly increased demand for computational power if the temporal correlation would be considered. Nevertheless, not only does the white noise assumption lead to an overoptimistic estimate of site velocity uncertainty, it also miscalculates the impact of offsets on the estimated site velocity uncertainty. Williams (2003a) examined the effect of offsets on the estimated velocity uncertainty, analytically for white noise and random walk (RW) noise, and numerically for flicker noise. He found that when the observational noise is assumed as white noise and N offsets are evenly distributed within a position time series, the estimated velocity uncertainty is highly sensitive to the occurrence of offsets, increasing by a factor of $N + 1$ when compared with the "offset-free" uncertainty. In contrast, neither the number nor the position of offsets significantly affects the estimated velocity uncertainty if the observational noise is RW. For the case of flicker noise, the effect of offsets on the velocity uncertainty is between the two end-members (Williams, 2003a). The effects of other types of noise processes and their mutual comparisons are yet unknown.

The noise contents of GNSS position time series are usually different site by site, and there is no universal noise model that is applicable to all the position time series. Current studies have shown that, although the combination of white noise plus flicker noise is the preferred noise model for the majority of the position time series, some stations can be better described by other models, including general power law model, Gauss-Markov model, and even RW (Santamaría-Gómez et al., 2011). The actual sensitivity of velocity uncertainty to offsets thus needs to be assessed on a site-by-site basis. The diverse noise types require identifying the determinant of the sensitivity and quantifying the dependence of the sensitivity on it.

In this study, in order to understand the impact of estimating offsets on the uncertainties of site velocity estimates, we develop a numerical method to assess the sensitivity of the velocity uncertainty estimate to offsets for different noise models and further determine the analytical dependence of the sensitivity on the deterministic indices characterizing the noise, including the correlation length of first-order Gauss-Markov (FOGM) model, the spectral index of power law noise, and the amplitude ratio between the flicker noise and white noise of a mixed model. This analysis enables the quantification and comparison of the sensitivities among different types of observational noise. In addition, we assess the sensitivity by analyzing actual GPS position time series. The sensitivity reflects the impact on reference frame stability when more position offsets would be detected or when new offsets occur. Since many offsets are induced by necessary site maintenance and updates, the sensitivity analysis has important practical implication for the operation and maintenance of continuous GNSS reference stations in order to meet the requirements on the accuracy and stability of future reference frame realizations.

2. Method

2.1. Power Law Noise Model

A common statistical model in geophysics is the power law noise whose power spectrum has the form

$$P_e(f) = P_0\left(\frac{f}{f_0}\right)^{\kappa}, \tag{1}$$

where f refers to frequency, P_0 and f_0 are normalization constants, and κ is called spectral index whose value typically is in the range of $-3 < \kappa < 1$ for geophysical phenomena (Agnew, 1992; Williams, 2003b; Zhang et al., 1997). The more negative the value of κ, the more dominant the low-frequency components are and thus more temporally correlated the noise is. The power law noise model is a RW when $\kappa = -2$, flicker noise when $\kappa = -1$, and white noise when $\kappa = 0$. The process is termed fractal RW when $-3 < \kappa < -1$ (Mandelbrot and Ness, 1968) and fractal white noise when $-1 < \kappa < 1$. The processes with $|\kappa| < 1$ are stationary. The noise with $\kappa \neq 0$ is temporally correlated and called red noise when $\kappa < 0$ and blue noise when $\kappa > 0$.

2.2. Velocity Uncertainty Estimation

The following regression model is typically adopted for analyzing site position time series:

$$y_t = c + r \cdot t + \sum_{i=1}^{K} b_i \cdot p_i + a_1 \cdot cos2\pi f_0 t + a_2 \cdot sin2\pi f_0 t + e_t, \tag{2}$$

where y_t is the site position coordinate observed at time t, having random observational noise e_t, and f_0=1 cpy ("cycle per year"). The parameters to be estimated include the constant term c, the linear velocity r, the annual amplitudes a_1 and a_2, and the magnitudes of total K offsets, which are denoted by $b_i (i = 1, \ldots, K)$. The Heaviside step function p_i is defined as

$$p_i = \begin{cases} 0 & \text{if } t < t_i \\ 1 & \text{if } t \geq t_i \end{cases}, \tag{3}$$

where t_i is the occurrence epoch of the i*th* offset. This is a general model that is applicable to both horizontal and vertical components. We thus do not discriminate among different position coordinate components.

Given the covariance matrix (C_x) of the observational noise, the least squares estimate of the unknown vector $\hat{\boldsymbol{x}} = \left[\hat{c}, \hat{r}, \hat{a}_1, \hat{a}_2, \hat{b}_1, \ldots, \hat{b}_K\right]^T$ is

$$\hat{\mathbf{x}} = \left[\mathbf{A^T C_x^{-1}} A\right]^{-1} A^T C_x^{-1} y, \tag{4}$$

and the posterior covariance matrix for the estimates is

$$\mathbf{C}_{\hat{\mathbf{x}}} = \left[\mathbf{A^T C_x^{-1}} A\right]^{-1}, \tag{5}$$

where

$$\mathbf{y} = \left[y_1, \ldots, y_n\right]^T, \tag{6}$$

and

$$\mathbf{A} = \begin{Bmatrix} 1 & t_1 & cos2\pi f_0 t_1 & sin2\pi f_0 t_1 & p_1 & \ldots & p_K \\ 1 & t_2 & cos2\pi f_0 t_2 & sin2\pi f_0 t_2 & p_1 & \ldots & p_K \\ \vdots & \vdots & & & & & \\ 1 & t_n & cos2\pi f_0 t_n & sin2\pi f_0 t_n & p_1 & \ldots & p_K \end{Bmatrix}. \tag{7}$$

As shown in equation (5), the uncertainty of the site velocity estimate depends on the noise of the position time series and the parameters estimated. We thus assess the impact of offsets on the velocity uncertainty estimate by assuming different models, which are commonly used to describe the noise in GNSS position time series and other geophysical signals, including (1) flicker noise; (2) the FOGM models with correlation lengths of 0.8, 5, 10, 20, 50, 120, 180, 360 and 600 days, respectively; (3) the fractal white noise models with $\kappa = -0.6$ and -0.8, respectively; (4) the fractal RWs with $\kappa = -1.4$ and -1.6; (5) white noise; and (6) the combinations of flicker noise and white noise with magnitude ratios of 1:4, 3:5, 5:3, and 4:1, respectively.

The ratio of 5:3 has been suggested by Mao et al. (1999) based on the analysis of the observations from 23 globally distributed GPS stations. For each noise type, the specific parameter values are chosen so that we have sufficient samples to fit an analytical expression (see following discussions).

Given their covariance matrix $\mathbf{C_e}$, the noise time series are synthesized by following the procedure described in section 2.3. For each noise type, we synthesize 400 noise time series, each one a decade long and with a daily sampling rate. In order to keep the statistical characters of the synthetic time series from different noise models consistent, we compute the root-mean-square (RMS) scatters for each simulated time series and scale the noise generating parameters so that the mean RMS of the 400 simulated time series equals 1 mm. The initial noise covariance matrix, which has been used to synthesize the original noise time series, is then normalized by using the same scale factor. In this way, we can obtain the covariance matrices for decade-long random errors, which are of different types, but have statistically equal RMS scatters in time. The velocity uncertainties associated with various noise models are then derived by using the normalized covariance matrices based on equation (5).

When the velocity is estimated together with offset magnitudes by least squares assuming the noise term is white noise, the maximum velocity uncertainty occurs when the offsets are evenly spaced over the entire time series (Williams, 2003b). This is still true when the annual terms are included in the estimation as well, except in the case that offsets occur annually. The annual occurrence of offsets prevents the precise estimation of annual signals and consequently degrades the precision of the velocity estimate. Based on our experiment, the estimated velocity uncertainty is exceptionally inflated by the annual occurrence of offsets, and this case will not be discussed in this study. In order to maximize the impact of estimating offsets on the standard deviation of the velocity estimate, we add parameters representing evenly spaced offsets within the decade-long time series for the estimation. We sequentially increase the number of offset parameters from 0 ("offset free") to 21 and estimate the velocity uncertainty at each step. The case of nine offset parameters is excluded because of the annual occurrence rate. The sensitivities of the velocity uncertainties to the addition of offset parameters are then compared among different noise models.

2.3. Colored Noise Realization

The noise time series e_t can be realized based on the eigen-decomposition of its covariance matrix $\mathbf{C_e}$ (Golub & Van, 2013):

$$\mathbf{C_e} = \mathbf{V} \cdot \mathbf{D} \cdot \mathbf{V^T}, \tag{8}$$

where $\mathbf{D}$ is the diagonal matrix of eigenvalues and each column of $\mathbf{V}$ is an eigenvector. If $\mathbf{w}$ represents a column vector of independent and identically distributed (IID) gaussian random variables with zero mean and unit variance, the product $\mathbf{e} = \mathbf{V} \cdot \mathbf{D}^{\frac{1}{2}} \cdot \mathbf{w}$ creates a realization of the noise described by the given covariance matrix, since

$$\mathbf{C_e} = \langle \mathbf{e} \cdot \mathbf{e^T} \rangle = \langle \mathbf{V} \cdot \mathbf{D}^{\frac{1}{2}} \cdot \mathbf{w} \cdot \mathbf{w^T} \cdot \mathbf{D}^{\frac{1}{2}} \cdot \mathbf{V^T} \rangle = \mathbf{V} \cdot \mathbf{D}^{\frac{1}{2}} \cdot \langle \mathbf{w} \cdot \mathbf{w^T} \rangle \cdot \mathbf{D}^{\frac{1}{2}} \cdot \mathbf{V^T} = \mathbf{V} \cdot \mathbf{D}^{\frac{1}{2}} \cdot \mathbf{I} \cdot \mathbf{D}^{\frac{1}{2}} \cdot \mathbf{V^T} = \mathbf{V} \cdot \mathbf{D} \cdot \mathbf{V^T}, \tag{9}$$

where the angle brackets $\langle\rangle$ denotes the expectation or infinite ensemble average and $\mathbf{I}$ is an identity matrix.

For a stationary noise process, its covariance matrix $\mathbf{C_e}$ can be conveniently constructed based on its autocorrelation function defined below (often the definition we use below is called the autocovariance function with autocorrelation referring to the autocovariance normalized by the variance of the process). An autocorrelation function, or simply correlation function, is defined for any noise process e_t as

$$\phi_e(t, \tau) = \langle e_t \cdot e_{t+\tau} \rangle = \lim_{T \to \infty} \frac{1}{T} \int_{-T/2}^{T/2} e_t \cdot e_{t+\tau} dt. \tag{10}$$

For a stationary process, the correlation function becomes invariant to the time shift τ and thus independent of time t, that is, $\phi_e(t, \tau) = \phi_e(\tau)$. In addition, the Fourier transform of the correlation function gives the power spectral density function (or simply power spectrum) of the stationary process:

$$P_e(f) = \int_{-\infty}^{+\infty} \phi_e(\tau) \cdot e^{-i2\pi f \tau} d\tau, \tag{11}$$

and the inverse transform reverts to the correlation function:

$$\phi_e(\tau) = \int_{-\infty}^{+\infty} P_e(f) \cdot e^{i2\pi f \tau} df. \tag{12}$$

Therefore, the correlation function of a stationary noise process can also be obtained from the power spectrum of the process.

However, the power spectrum of the power law noise, as given in equation (1), is not integrable unless $|\kappa| < 1$ and therefore, strictly speaking, does not constitute a valid power spectrum in the theory of stationary stochastic processes. For $\kappa \leq -1$, the lack of integrability resulting from the rapid increase at low frequency is called "infrared catastrophe' (Wornell, 1993). In fact, the stochastic process is stationary when $\kappa > -1$ and nonstationary when $\kappa < -1$ Kasdin (1995, and references therein). For nonstationary processes, the correlation function as defined in equation (10) depends not only on the time interval τ but also on the time t, and the power spectrum of the process is not defined. Thus, in the expression of the power spectrum for power law noise, an apparent contradiction exists between the stationarity assumption upon which usual spectral concepts are based and the fact that such spectral expression cannot be associated with a˜ stationary process.

However, in practice, the paradox is resolved because observations are always band limited due to finite span and discrete sampling and thus render us capable of avoiding the nonintegrable singularities implied by the ideal mathematical model. We can always obtain a finite-power noise time series, whose power spectrum is well defined and follows the power law. Consequently, the correlation function of this finite-power power law process can be obtained by applying the Inverse Fourier Transform (IFT) to the power spectrum.

Due to the dilemma discussed above, there have been a number of subtleties arising in the development of the covariance for the $1/f$ spectral behavior. For example, Zhang et al. (1997) provide a flicker noise covariance matrix that is derived based on an algorithm by Gardner (1978) (Williams et al., 2004). In addition, Williams (2003a) constructs a flicker noise covariance matrix based on a transformation matrix given by Hosking (1981), the derivation of which uses the fractional differencing/integrating method. Thus, we also compare these three covariance matrices generated by different methods: the first one, referred to Flicker-I, is generated by the IFT of the $1/f$ power spectrum, as discussed above; Flicker-II and Flicker-III are the covariance matrices given by Zhang et al. (1997) and Williams (2003a), respectively. We focus on whether or not the different forms of covariance matrix for flicker noise would significantly alter the velocity uncertainty estimate.

Figure 1 shows the samples of the synthesized noise time series of different types.

2.4. The Zero-Frequency Component of Power Spectrum

The correlation function can be obtained by applying the IFT to the power spectrum of the noise that always has finite power in practice. Before applying the IFT to obtain the correlation function, we set the discrete power spectrum value at $f = 0$ (i.e., $P_e(0)$) to be 0 mm^2/cpy for the decade-long noise series. This is equivalent to removing the mean values μ_e of the noise before any statistical analysis.

Assigning different values to $P_e(0)$ only changes the variance of the mean of the noise samples but does not alter the correlation statistics once the mean has been removed. For a noise time series with N values, since its power spectrum $P_e(k)$ and correlation function $\phi_e(\tau)$ are a Fourier transform pair, their relation is given by the Parseval's theorem (Titchmarsh, 1968):

$$\frac{1}{N}\sum_{k=0}^{N-1} P_e(k)^2 = \sum_{\tau=0}^{N-1} \phi_e(\tau)^2. \tag{13}$$

It can be seen from equation (13) that a zero-frequency component change of $\Delta P_e(0)$ offsets the correlation function by $\Delta\phi_e = \Delta P_e(0)/N$. Figure 2a compares the correlation functions of the decade-long daily flicker noise having different $P_e(0)$ values. They are obtained by applying the IFT to the $1/f$ spectra whose zero-frequency components are modified to different values. It can be seen from Figure 2a that when the value of $P_e(0)$ is increased from 0 mm^2/cpy to 10,000 mm^2/cpy and 30,000 mm^2/cpy, the correlation function is shifted by $\Delta\phi_x = 10,000/(2\times 3,652-1) = 1.37$ mm^2 and $\Delta\phi_x = 30,000/(2\times 3,652-1) = 4.11$ mm^2, respectively. Figure 2b shows three sample noise time series synthesized by using the three modified power spectra.

Larger $P_e(0)$ value implies larger variance of the mean of the realized random noise, but the estimated velocity uncertainties are always the same independent of the values assigned to $P_e(0)$. Take the offset-free case for example. Although the covariance matrices constructed from the correlation functions shown in Figure 2a

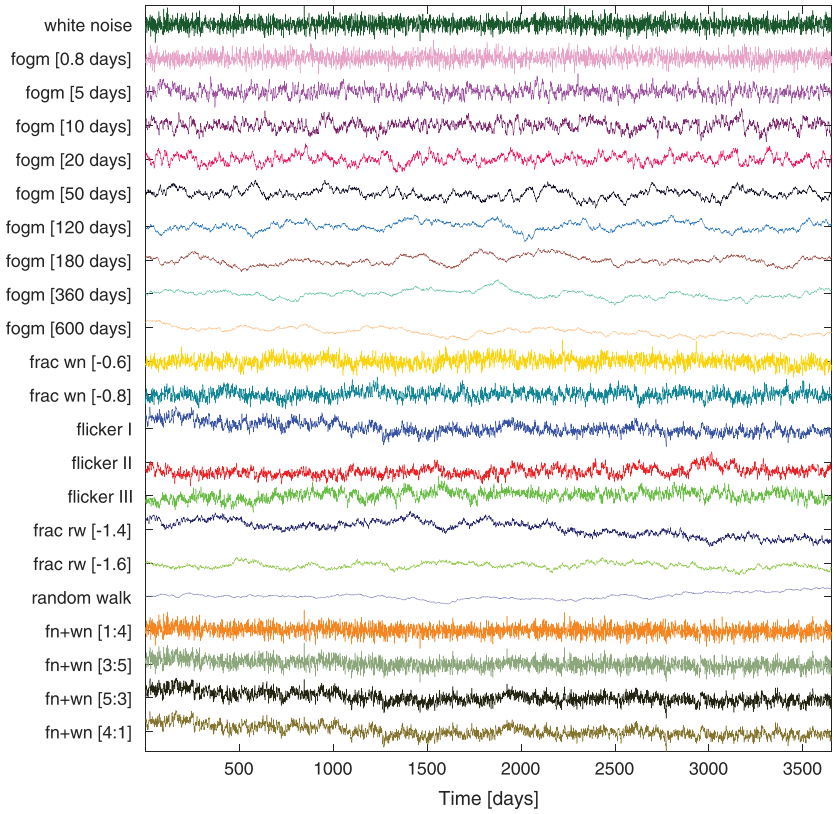

Figure 1. Samples of the simulated noise time series of different types, including white noise (wn), first-order Gauss-Markov (fogm) noise, fractal white niose (frac wn), flicker noise, fractal random walk (frac rw), random walk, and the mixture of white noise and flick noise (fn+wn). For each noise type, the mean RMS of the 400 simulated time series is 1 mm.

are different, the estimated sigmas for the parameters of r, a_1, and a_2 are all the same, having the values of 0.27 mm/yr and 0.31 and 0.31 mm, respectively. Meanwhile, different $P_e(0)$ values do produce different sigma estimates for the constant term c, which are 1.46, 1.87, and 2.50 mm when $P_e(0)$ takes the values of 0 mm^2/cpy, 10,000 mm^2/cpy and 30,000 mm^2/cpy, respectively.

3. Results

3.1. Analysis of Simulated Data

In Figure 3a, the velocity uncertainties, estimated by assuming different noise models, are plotted against the number of parameters representing evenly space offsets within a decade-long daily position time series. The results are also listed in Table A1. It can be seen that the correlated noise models always produce larger velocity uncertainties than the white noise model when there is no offset parameter in the estimation. For example, the estimated velocity uncertainty for the white noise model is 0.006 mm/yr, whereas the value is 0.092 mm/yr for the Flick I model, about 15.3 times greater, even though both noise time series have the same RMS scatter of the residuals. When parameters are added representing evenly spaced offsets into the analysis of the noise time series, the estimated velocity uncertainty grows as the number of offset parameters increases for all the noise models. As shown in Figure 3a, when the number of offset parameters is less than 17, the correlated noise models being tested induce greater velocity uncertainties than that associated with the white noise. However, as the number of offset parameters further grows, the velocity uncertainties for the white noise starts to exceed those for the correlated noise models.

For flicker noise, we compare three different covariance forms as discussed in section 2. Among the three different covariances, the Flicker-II and Flicker-III produce the maximal and minimal velocity uncertainties respectively, while the velocity uncertainties associated with the Flicker-I are in between. The differences

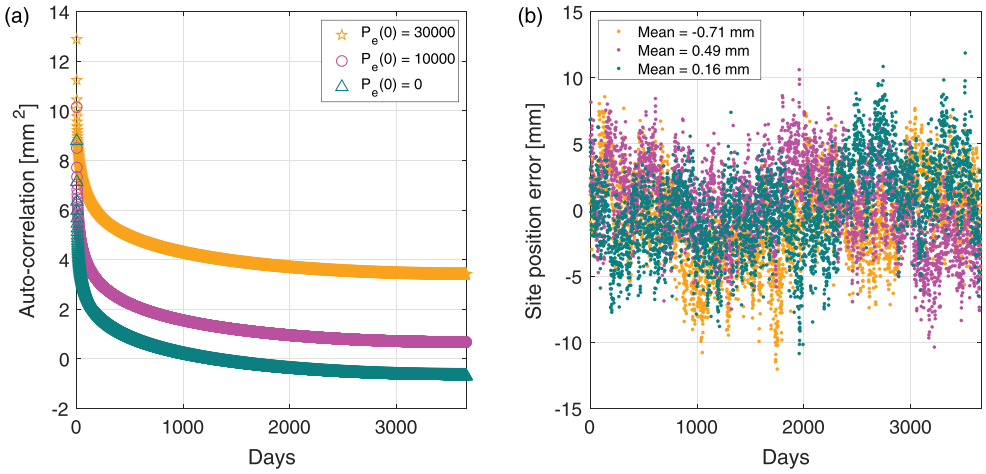

Figure 2. (a) The autocorrelation functions generated by the IFT of the $1/f$ power spectrum, whose zero-frequency value $P_e(0)$ is set to be 0 mm^2/cpy, 10,000 mm^2/cpy, and 30,000 mm^2/cpy, respectively. (b) The sample flicker noise time series synthesized based on the three modified power spectra. The mean values are compared among the three samples, illustrating that greater $P_e(0)$ is more likely to produce a random realization with larger mean value.

in the estimated velocity uncertainties between Flicker-II and Flicker-III decrease as the number of offset parameters increases. The maximal difference is 0.005 mm/yr, which is less than one tenth of the uncertainty magnitude by assuming flicker noise. Thus, the differences among the three covariances have negligible impact on the velocity uncertainty assessment for flicker noise.

For each given number of offset parameters, we can calculate an inflation factor as the ratio of the estimated velocity uncertainty to the "offset-free" velocity uncertainty. The results are listed in Table A2 and shown in Figure 3b for all the noise models. For a given number of offset parameters, the calculated

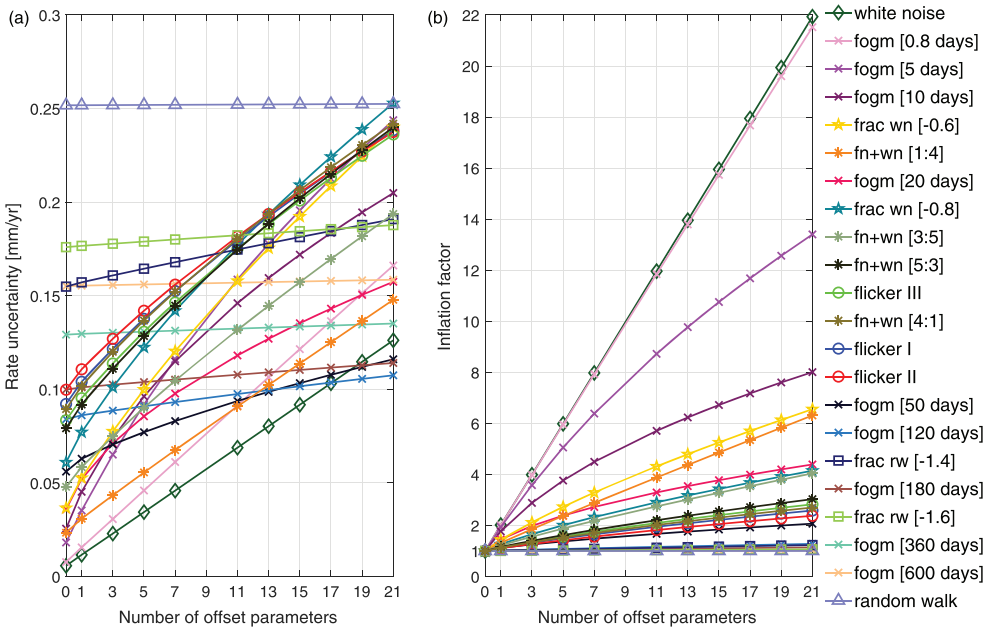

Figure 3. (a) Velocity uncertainties estimated using different noise models when the number of parameters representing evenly spaced offsets increases from 0 to 21 for a decade-long daily noise time series. (b) Similar to (a), except that for each noise model, the uncertainties are divided by the uncertainty when there is no offset parameter in the estimation ("offset free"). Such ratio is defined as the inflation factor, reflecting how many times the uncertainty with offset parameters is greater than the "offset-free" uncertainty. The noise models in the legend are arranged in descending order of the sensitivity of the velocity uncertainty to estimating offsets.

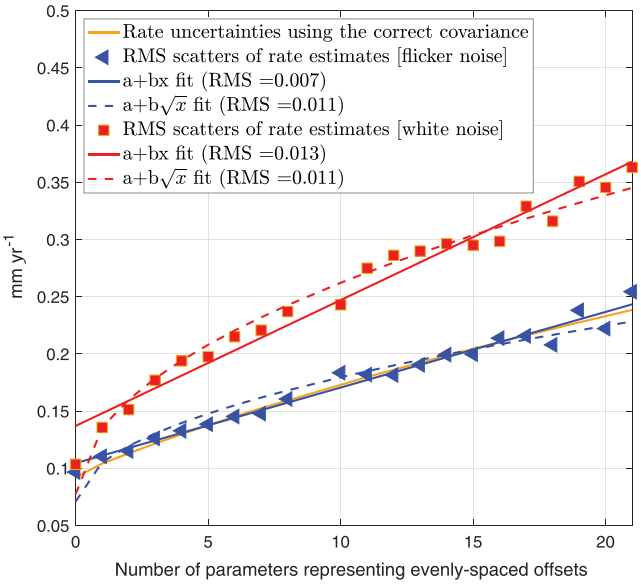

Figure 4. Comparison between the analytical forms of $a + bx$ and $a + b\sqrt{x}$ for fitting the increase of velocity uncertainties with the addition of offset parameters. The observational noise is assumed to be flicker noise.

inflation factors are different for the noise models. The white noise and the RW noise show the maximum and minimum uncertainty inflations, respectively. The velocity uncertainty grows by a factor of 22 when 21 offset parameters are included in the estimation assuming the white noise, consistent with that concluded by Williams (2003a). In contrast, the uncertainty growth in the RW case is so marginal, only by a factor of 1.3 when the number of offset parameters increases from 0 to 21, that it can be barely seen in Figure 3b. That is, the strong temporal correlation in RW noise enlarges the uncertainty of the velocity estimate on the one hand and mitigates the impact of estimating offsets on velocity uncertainties on the other hand. Figure 3b also shows that the inflation factors increase with the addition of offset parameters for all the noise models. The inflation factors and the velocity uncertainties are almost linearly proportional to the number of offsets. This disagrees with the dependence form of $a + b\sqrt{x}$ (where x is number of offset parameters) as suggested by Griffiths and Ray (2016). Comparing the RMS of residuals, we find that the linear fit ($a + bx$) always outperforms the square-root form ($a + b\sqrt{x}$) for all the noise models, except the FOMG models with correlation length of 10 and 20 days. In the case of flicker noise, for a given number of offsets, we calculate the RMS scatters of the velocity estimates for the 400 simulated noise time series. As shown in Figure 4, these RMS values closely follows the velocity uncertainties associated with the flicker noise as the number of offsets increases. The linear fit results in a much smaller RMS of residuals (0.007 mm/yr) than that of the square-root fit (0.011 mm/yr). However, if the assumption of white noise is made in the velocity estimation, we always obtain larger velocity RMSs than those calculated by using the correct noise covariance matrix, and the white noise estimates are better fitted by the square-root model, particularly when the number of offsets is less than 5. Therefore, the white noise assumption in the estimation of site velocities by Griffiths and Ray (2016) would explain why they obtain the dependence of the square-root form. Figure 4 also shows that estimating with the white noise assumption in the presence of the correlated noise increases the impact of offsets. More detailed discussions can be found in section 4.

For each of the noise models in Figure 3b, we fit a linear trend to the inflation factors, which reflects the rate of increase of the inflation factor as the number of offset parameters grows and thus measures the sensitivity of the velocity uncertainty to offsets. Although the linear model does not necessarily represent the best fit for the 10- and 20-day FOGM models, the fitted linear trends represent the average sensitivity for these two models. The fitted linear trends for all the noise models are listed in Table A2.

Figure 5 compares the sensitivities for all the noise models. The white noise exhibits the greatest sensitivity; the inflation factor increases by 0.996 every time a new offset parameter is added. In other words, every additional offset parameter increases the velocity uncertainty by 99.6% of the "offset-free" value. As can be seen from Figure 5 and Table A2, the sensitivity decays when the noise becomes more temporally correlated, and different noise types show different decay characteristics. For the FOGM models, the sensitivity (s) decays as the correlation length (l) increases, from 0.996 when the correlation length is 0 day (i.e., white noise) to 0.001 when the correlation length increases to 600 days. The decay can be well described by a power law form, $s(l) \propto l^{\alpha}$, with $\alpha = -1.34$; For the power law noise, the sensitivity decreases as the spectral index κ becomes more negative. When κ decreases from 0 (white noise) to -2 (RW), the sensitivity decreases from 0.996 to 0.0001. The decay follows the form of the normal distribution, that is, $s(\kappa) \propto e^{-\kappa^2/2\sigma^2}$ with σ estimated to be 0.45. For the mixture of flicker noise and white noise, the sensitivity decays as the percentage (p) of the flicker noise amplitude increases. The decay also follows the power law form $s(p) \propto p^{\alpha}$ with α estimated to be -0.78. Figure 5 thus allows the quantitative assessment of the impact of offsets on site velocity uncertainties for different noise models, as well as the mutual comparisons among them. For example, as shown in Figure 5, the power law noise with $\kappa = -0.8$, the combined model with the amplitude ratio of 3:5 between the flicker noise and the white noise, and the FOGM with the correlation length of about 20 days result in the similar sensitivities to offsets. Figure 5 also shows that the sensitivity of flicker noise is comparable to that of the FOGM model with the correlation length of about 30 days.

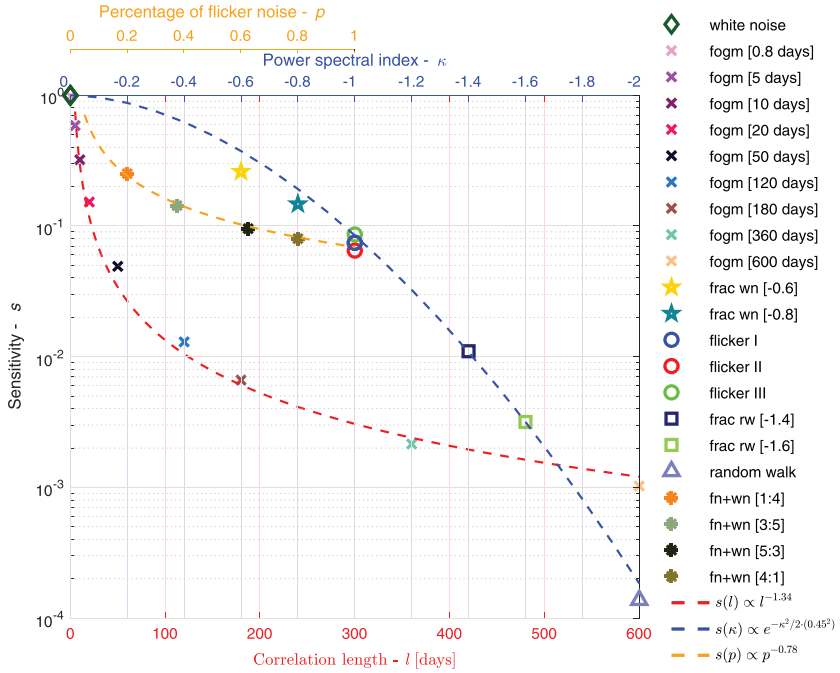

Figure 5. The sensitivities of rate uncertainty to offsets for different noise models. For the FOGM models, the power law models and the combined models of flicker noise and white noise and the sensitivities (s) are plotted against the correlation length (l) in red, the power spectral index (κ) in blue, and the percentage of the flicker noise amplitude (p) in orange, respectively. The dashed lines indicate the fitted analytical forms describing the sensitivity decay for different noise types.

Although the simulation analysis is based on the decade-long time series, it can be shown that, for white and RW noise, when the length of the time series is much larger than the number of offsets, the sensitivity does not change. For other noise models, the sensitivity derived by analyzing GPS position time series having the average length of 14 years is consistent with the simulation study based on decade-long time series (see section 3.2).

3.2. Analysis of Plate Boundary Observatory results

We have evaluated the inferences from section 3.1 by analysis of the geodetic time series available from the Plate Boundary Observatory (PBO) based in North America (Herring et al., 2016). We analyzed the combined PBO position time series available through UNAVCO for the period 1 January 1996 to 15 September 2018. This period covers all the combined GPS products available for PBO. We restricted our analysis to the 1954 sites with more than 10 years of data. For each of these time series, we added between 1 and 19 offset parameters, uniformly spaced, to the existing parameterization of these time series, and reanalyzed the time series using the standard processing methods discussed in (Herring et al., 2016). The existing parameterizations included offsets for antenna and radome changes, earthquakes with possible postseismic log time dependence, and offsets that had been visually identified in the time series. The correlated noise modeling was based on the first-order Gauss-Markov Extrapolation (FOGMEX) algorithm discussed and analyzed in Floyd and Herring (2019). This algorithm uses the dependence of the χ^2 per degree of freedom of means of time series residuals over successively longer averaging times to infer the long-term correlated noise characteristics. The algorithm can either rescale parameter standard deviations from a white noise weighted least squares solution or estimate the parameters with a Kalman filter with a RW process noise value determined such that the standard deviation of the velocity estimate matches the rescaled white noise weighted least squares solution. Since the noise characterization algorithm uses residuals to a time series fit, the RW process noise will change as offset parameters are added and so for individual time series, the standard deviations of the velocity estimates may increase or decrease as offset parameters are added. In order to examine the overall characteristics of the impact of adding offset parameters, we used medians of statistical properties in bins of 150 stations after the stations had been sorted by their RW process noise values. The choice

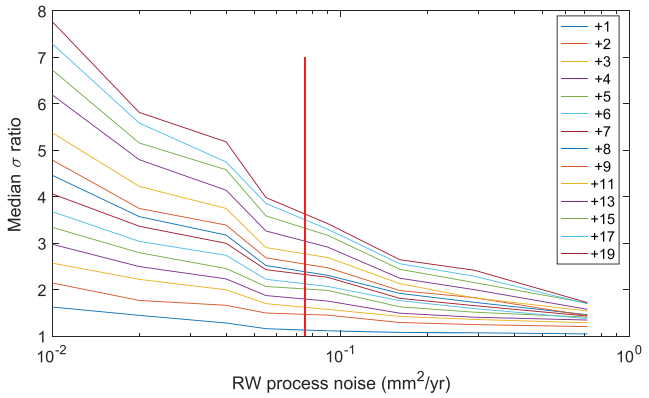

Figure 6. Median values of the ratio of the velocity estimate standard deviation from the Kalman filter analysis with the number of offset parameters added shown in the legend to the velocity estimate standard deviation when no additional offset parameters are added as a function of the median random walk (RW) process noise values in bins of 150 stations when the stations are sorted by increasing process noise. The vertical red line is the median process noise value for the 1954 PBO stations analyzed.

of 150-station bin was a compromise between having a reasonable number of bins for the RW process noise characteristics and averaging the station-to-station variability due to individual realizations.

We show the two main results from this analysis in Figures 6 and 7. We examine two basic statistics (1) medians of the ratio of velocity standard deviation with added offset parameters to the standard deviation with no additional offsets (Figure 6) and (2) the ratio of the absolute value of the change in the velocity estimate, when offset parameters are added, to the velocity standard deviation of the velocity estimate with the added offset parameters (Figure 7). These values are shown as function of RW process noise. Small values of the RW process noise correspond to processes dominated by white noise. For white noise, the results in Figure 3 show that the velocity estimate standard deviation should increase proportionally with the number of offsets. The times series analyzed here had a median value of 1.6 offsets per time series with the average length of the time series being almost 14 years. The values in Figure 6 at small values of the RW process noise are similar to the noise simulations once the initial number of offsets already in the time series is accounted for. At the median value of 0.08 mm^2/yr RW process noise for the PBO time series, Figure 6 shows only a 14% increase in the standard deviation of the velocity if an additional offset is added to the middle of the existing time series. Offsets in the middle of the time series have the most impact and hence this value is an upper bound on the effects of adding a new offset.

In addition to analyzing the changes in the standard deviations of the velocity estimates, we also examined the changes in the velocity estimates themselves when offset parameters were added. The medians of the absolute values of the change in velocity estimate from its initial estimate when between 1 and 19 parameters representing uniformly spaced offsets are added divided by the standard deviation of the estimate with the added offsets are shown in Figure 7. The standard deviations of the velocity estimates with one added offset parameter are shown on the right axis in this figure. We see from the figure that at larger values of the process noise values (more temporally correlated time series) the changes in velocity estimates are consistent with the standard deviations of the estimates but at smaller values of the process noise the changes are larger than would be expected given the standard deviations of the estimates. At the median value of the process noise, the changes are about twice the size expected based on the standard deviations independent of the number of offsets. (The velocity changes increase with the number of offsets proportional to the standard deviation of the estimates). The factor of two difference between the changes and their standard deviations is consistent with the conclusion of Floyd and Herring (2019) that the FOGMEX algorithm underestimates

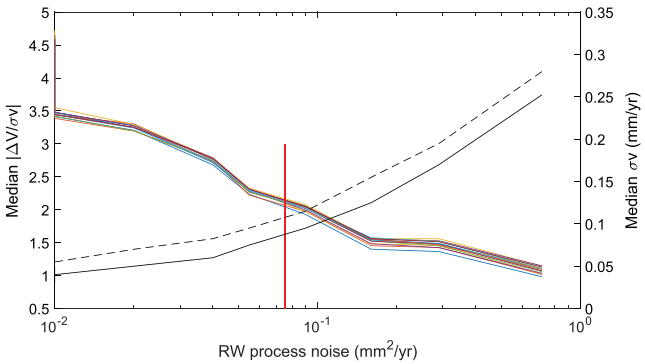

Figure 7. Left axis, ratio of the median values of the absolute value of velocity estimate changes from the Kalman filter analysis and the standard deviation of the velocity estimate with the additional offset parameters added according to the legend in Figure 6 shown as a function the median random walk (RW) process noise values as defined in Figure 6. Right axis and black lines show the median velocity estimate standard deviation with no additional offsets (solid line) and with one additional offset in the center of the time series (dashed line).

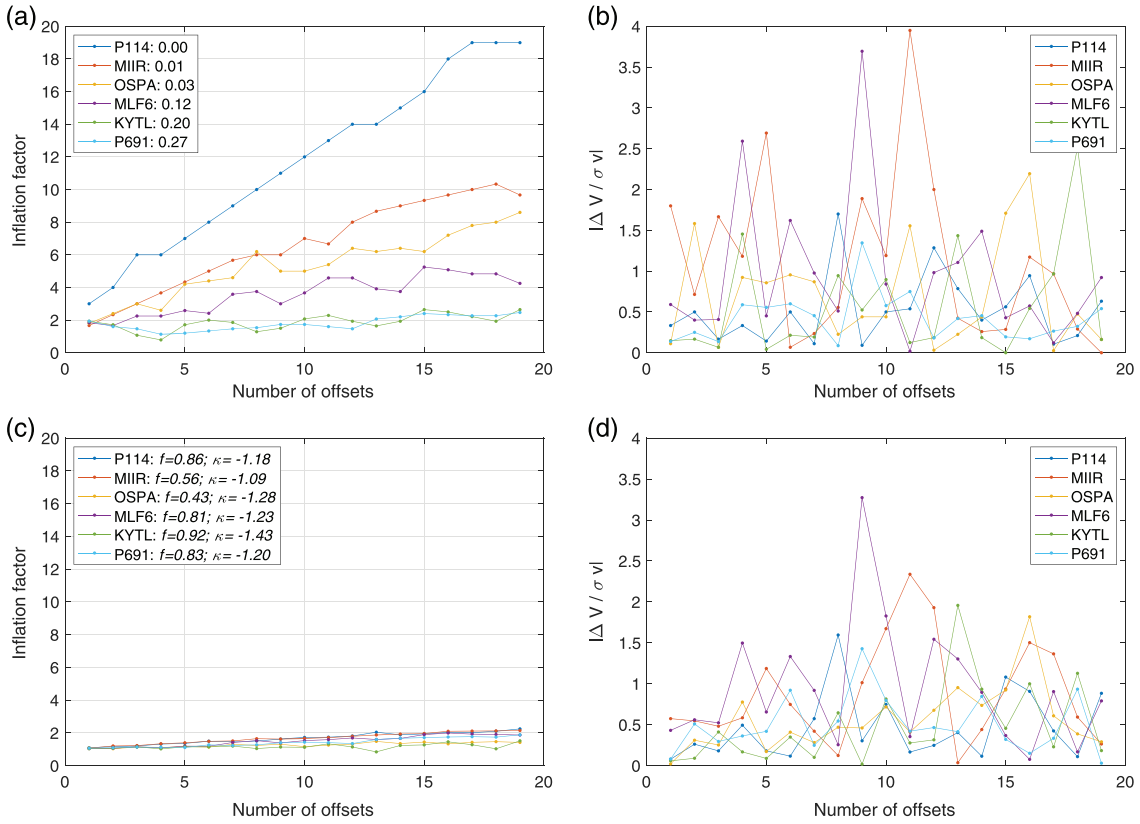

Figure 8. (a) The ratio between the velocity estimate standard deviations with and without additional offset parameters, analyzed based on the FOGMEX method for six sites whose RW process noise values in the north component are the 10%, 40%, 60%, 85%, 90%, and 92% quantiles of all the PBO sites we analyzed. (b) The ratio of the absolute value of velocity estimate changes from the FOGMEX analysis to the standard deviation of the velocity estimate with additional offset parameters added. (c) The same as (a) but analyzed using the MLE method. The inferred best noise model is the combination of power law noise and white noise, with the power index of κ and the white noise fraction of f. (d) The same as (b) but analyzed using the MLE method.

the velocity standard deviations when the process noise is a combination of flicker and white noise. Since the rescaling of the FOGMEX standard deviations would be applied across all analyses and does not depend on the number of offset parameters added, the conclusion from Figure 6 of the changes in standard deviations remains valid. The underestimation of the standard deviation is more pronounced for small values of the process noise where white noise dominates. For the PBO time series, adding an additional offset, at the middle of the times series, will change the velocity estimates by about 0.11 mm/yr. This value is computed from the difference of the velocity estimate variances with no offsets and one added offset, scaled by the ratio of the absolute velocity changes divided by their standard deviations at the median value. Offsets added at other times will have less impact of the velocity estimates.

Figure 8 shows the results of representative sites with different RW process noise values in the north component. Consistent with the results shown in Figure 6, when additional offset parameters are successively added in the estimation, the rate of increase of the velocity standard deviation becomes smaller as the RW process noise value (i.e., the degree of temporal correlation) increases. In addition, as shown in Figure 8b, when additional offset parameters are added, the ratio of the changes in velocity estimate to the standard deviations of the velocity estimate does not show obvious dependence on the number of offsets added.

Besides the FOGMEX technique, we also use the Maximum Likelihood Estimation (MLE) technique, as implemented by Bos et al. (2013), to estimate the optimal noise model for the representative sites, based on which the impact of estimating offsets is further assessed. We compare six different noise models, including (1) white noise, (2) flicker noise, (3) RW noise, (4) power law noise, (5) the combination of flicker noise and white noise, and (6) the combination of power law noise and white noise. The noise model with the

minimum Akaike Information Criteria is selected as the best noise model used for the velocity estimation. For all the sites we analyzed, the combination of power law noise and white noise always represents the best noise model, although the estimated fraction of the white noise component and the power index κ are different from site to site. As shown in Figure 8c, the velocity estimate standard deviations, which are derived based on the MLE-inferred best noise models, are less sensitive to the inclusion of additional offset parameters when compared with the FOGMEX analysis, particularly for the sites with small RW process noise values. It would suggests that MLE-inferred correlations are even more important than implied by the FOGMEX analysis and might also explain why the FOGMEX underestimate the standard deviations of velocity changes with added offsets by a factor of 3.5, compared to 2 at the median RW process noise. Therefore, instead of analyzing all the PBO time series using the MLE, which would be time consuming, we consider the result of the fast FOGMEX analysis as the upper bound on the impact of estimating offsets. As shown in Figure 8c, once an additional offset parameter is added to the middle of the time series, the increases in the velocity standard deviation are 10%, 7%, 8%, 5%, 4%, and 8%, respectively, for the six sites we analyzed, consistent with the FOGMEX results at the median RW process noise value. The ratio of the changes in velocity estimate to velocity estimate standard deviations has a median value of 0.6 (Figure 8d).

4. Discussion

Griffiths and Ray (2016) assess the impact of GNSS position offsets on station velocity uncertainties by analyzing the position time series of IGb08 reference stations. They conclude that the present level of position offsets in the IGS operational products, which is 0.9 offsets per site per decade, has great impact on all three components of the site velocity estimates. Particularly for the vertical component, compared with the ideal situation if no offsets existed in the IGS time series, the current IGS official offsets increase the WRMS scatter of the velocity estimates to 0.34 mm/yr on average, which is 30% larger than the mean formal error. They also conclude that if the number of offsets doubles, which is likely considering that the updated detection approach for the IGS second reprocessing increases the average number of offsets to 1.8 per station, the WRMS will increase by 40% to 0.48 mm/yr.

In Griffiths and Ray (2016), the site velocity, together with station coordinates and daily Earth Orientation Parameters (EOPs), is estimated by stacking weekly geocentric station coordinates and daily EOPs estimates using the CATREF software developed for the ITRF combinations (Altamimi et al., 2002). However, during the stacking, the temporal correlation of the position noise has not been accounted for. The approach thus overestimates the impact on the site velocity uncertainties as the number of offsets increases, as shown in Figure 4.

Based on our analysis, the temporal correlation within GPS site position noise considerably reduces the impact of estimating offsets on the estimated site velocity uncertainties. For a decade-long daily position time series, the white noise leads to the greatest increase of 48% (from 0.012 to 0.017 mm/yr) in the velocity uncertainty after doubling the number of offsets from 1 offset at the middle of the time series to 2 evenly spaced offsets. This result is more consistent with that of Griffiths and Ray (2016) since the temporal correlation of the observational noise has not been accounted for in their analysis. For all the correlated noise models, the temporal correlations greatly reduce the sensitivities to offsets when the correct noise covariance matrices are used.

In addition, our results show that in general the estimated velocity uncertainties vary proportionally with the number of offsets x, rather than $\sqrt{x}$ as suggested by Griffiths and Ray (2016), for all the noise models except the 10- and 20-day FOGM models. As shown in Figure 4, the square-root fit could result from the simplified white noise assumption in the site velocity estimation. Based on the fitted square-root function, Griffiths and Ray (2016) extrapolate the site velocity RMS (which is used to measure the velocity uncertainty) if no offsets existed in the IGS site position time series and conclude that the current number of offsets increases the site velocity uncertainty by 0.34 mm/yr in the vertical component. However, as shown in Figure 4, their analysis could overestimate the impact.

Almost all analyses of GNSS data sets show that a more appropriate model characterizing the noise in GNSS position time series would be closer to a combination of flicker noise plus white noise. For the flicker noise itself, doubling the number of offsets (from a single offset at the middle of the time series to 2 evenly spaced offsets) within the decade-long time series results in an increase of the velocity uncertainty estimate by 8.7%, that is, from 0.104 to 0.113 mm/yr. When the flicker noise is mixed with white noise, the velocity uncertainty estimate remains insensitive to offsets unless the white noise component dominates. For example, for the mixed model with the flicker-to-white noise amplitude ratio of 5:3, which is suggested by

Mao et al. (1999), the rate uncertainty increases by 11% (increases from 0.092 to 0.102 mm/yr) after the number of offsets increases from 1 to 2, slightly greater than the result of the pure flicker noise. When the white noise component increases such that flicker-to-white noise amplitude ratio is 3:5, the velocity uncertainty estimate becomes more sensitive to the number of offsets, increasing by 14% (from 0.059 to 0.067 mm/yr) when the number of offsets increases from 1 to 2. Nevertheless, the estimated inflations of the velocity uncertainties for both cases (flicker noise dominates vs. white noise dominates) are much smaller than the inflation of 40% estimated by Griffiths and Ray (2016) if the number of offsets doubles in the future. Furthermore, based on the analysis of PBO site time series, we found that adding one additional offset would increase the median velocity standard deviation by 14%, consistent with the conclusion of the simulation study.

One recommendation by Griffiths and Ray (2016) is the strict configuration control at IGS reference frame stations in order to limit the impact of potentially induced offsets on site velocity uncertainty estimates. However, the equipment replacement, such as replacing an old antenna with a newer model that allows the full GNSS frequency band to be observed, is critical to improve the overall GNSS data quality. Our study shows that, given the current level of noise correlation, the addition of offsets has limited impact on site velocity uncertainty if the correct noise covariance matrix is used. It is still practical to try to carefully measure the offset due to equipment changes by making local measurements before and after the equipment change. The necessary equipment update would only improve the site velocity estimation and thus the reference frame stability.

Our conclusions are based on using the correct covariance of the correlated noise in the estimation, which is computationally intensive. If the estimation assumes white noise despite the presence of correlated noise, as implemented by the programs such as CATREF and GLBOK, the assessed impact of offsets is still not as large as when the observational noise is purely white noise.

5. Conclusion

In order to meet the demands for monitoring long-term variations of the Earth system (e.g., tectonic deformations, sea level changes, temporal gravity variations etc.), the geodetic community is striving to realize and maintain a reference frame with accuracy at the level of 1 mm and stability at the level of 0.1 mm/yr (Gross et al., 2009). Future reprocessings of reference station data need account for new position offsets, which would be detected by improved detection algorithm or induced by earthquakes and necessary station maintenance. It is thus important to understand how offsets in GNSS position time series affect the accurate reference frame realization.

For all noise types, uncertainties of site velocity estimates increase as the number of offsets increases. When a decade-long daily position time series is analyzed, for all the noise models studied in this work except the 10- and 20-day FOGM models, the estimated velocity uncertainty increases proportionally to the number of position offsets. How fast the uncertainty increases depends on the degree of temporal correlation of the noise. The more temporally correlated the noise is the less sensitive the estimated velocity uncertainty is to offsets. The uncorrelated white noise yields the greatest uncertainty inflation rate as the number of offsets increases. For a decade-long daily time series, every additional offset increases the velocity uncertainty by 99.6% of the value when no offset exists. In contrast, for RW noise, in which any pair of errors is correlated however far apart they are in time, the velocity uncertainty only increases by 0.01% of the "offset-free" value per extra offset. The dependence of the sensitivity on the degree of correlation can be described by using analytical expressions. For FOGM models, the sensitivity decays as the correlation length increases, following a power law form. For power law noise models, the sensitivity decays as the power spectral index becomes more negative, following the decaying form of a normal distribution, and for the combination of flicker noise and white noise, the sensitivity decays with the increasing percentage of flicker noise amplitude, following a power law form.

It has long been known that GNSS position noise is temporally correlated, and the simplified assumption of white noise significantly underestimates the velocity uncertainty. Our results show that the white noise assumption overestimates the impact of position offsets on velocity uncertainty estimates as well. Based on the analyses of typical GPS position time series, the best model describing the position noise is the combination of flicker noise plus white noise. When the flicker-to-white noise amplitude ratio is 5:3 Mao et al. (1999), increasing the number of offsets from 1 to 2 only inflates the velocity uncertainty by 11%, which is much smaller than the increase of 40%, which is estimated by neglecting the temporal correlation of the

noise Griffiths and Ray (2016). Based on the analysis of 1954 PBO position time series, we find that adding one additional offset to the PBO time series would increase the median velocity standard deviation by 14%. The impact of offsets depends on the noise type, but not on the noise magnitude. Since there is no significant difference in the spectral characteristics of north, east, and vertical component noise (Mao et al., 1999), the estimated impact of offsets would be the same for all three position components.

In conclusion, the temporal correlation, which commonly exists among GNSS site position noise, considerably mitigates the impact of position offsets on site velocity uncertainties when the correct covariance matrix is used in estimation. The simplified assumption of white noise overestimates the impact of offsets. Thus, the existence and potential addition of position offsets will not significantly undermine the stability of reference frame realizations until the temporal correlation of GNSS position noise could be reduced sufficiently. Our results suggest that, in current efforts of high-quality reference frame realization, it is unnecessary to excessively limit position offsets, which are often inevitably induced by earthquakes or the necessary site maintenance/updates ensuring high-quality observations. Instead, it is critical to reduce the temporal correlation of GNSS position noise through improved modelings of nonlinear site motions, the orbit, atmospheric delays, multipath mitigation, antenna/receiver updates and so on.

Appendix A

In the appendix, we include the estimated velocity uncertainties associated with different noise models by assuming different numbers of offsets within a decadelong daily position time series (Table A1). We also include in Table A2 the velocity uncertainty inflation factors, which are calculated as the ratio of the velocity uncertainty estimate with offsets to that without offsets for a given noise model.

Table A1
Estimated velocity uncertainties (in unit of mmyr^{-1}) by assuming different noise models for a decade-long daily position time series

	# of offset parameters										
Model	0	1	3	5	7	11	13	15	17	19	21
white noise	0.006	0.012	0.023	0.034	0.046	0.069	0.080	0.092	0.103	0.115	0.126
fogm [0.8 days]	0.008	0.016	0.031	0.046	0.061	0.091	0.106	0.121	0.136	0.151	0.166
fogm [5 days]	0.018	0.035	0.065	0.092	0.116	0.159	0.178	0.196	0.213	0.229	0.244
fogm [10 days]	0.026	0.045	0.074	0.096	0.115	0.146	0.159	0.172	0.184	0.195	0.205
fogm [20 days]	0.036	0.052	0.071	0.086	0.098	0.118	0.127	0.135	0.143	0.150	0.157
fogm [50 days]	0.056	0.063	0.071	0.077	0.083	0.094	0.099	0.103	0.108	0.112	0.116
fogm [120 days]	0.084	0.086	0.089	0.091	0.093	0.098	0.100	0.102	0.104	0.106	0.108
fogm [180 days]	0.100	0.101	0.103	0.104	0.105	0.108	0.109	0.110	0.112	0.113	0.114
fogm [360 days]	0.129	0.130	0.130	0.131	0.131	0.132	0.133	0.134	0.134	0.135	0.135
fogm [600 days]	0.155	0.155	0.156	0.156	0.156	0.157	0.157	0.158	0.158	0.158	0.159
frac wn [-0.6]	0.037	0.053	0.078	0.100	0.120	0.158	0.175	0.192	0.209	0.225	0.240
frac wn [-0.8]	0.061	0.077	0.101	0.122	0.142	0.177	0.194	0.209	0.224	0.239	0.253
flicker I	0.092	0.104	0.122	0.138	0.152	0.180	0.192	0.204	0.216	0.227	0.238
flicker II	0.100	0.111	0.127	0.142	0.156	0.182	0.194	0.205	0.216	0.227	0.238
flicker III	0.083	0.095	0.114	0.131	0.146	0.175	0.188	0.201	0.213	0.225	0.236
frac rw [-1.4]	0.155	0.157	0.161	0.164	0.168	0.175	0.178	0.181	0.185	0.188	0.191
frac rw [-1.6]	0.176	0.177	0.178	0.179	0.180	0.182	0.183	0.184	0.186	0.187	0.188
random walk	0.252	0.252	0.252	0.252	0.252	0.252	0.252	0.252	0.252	0.252	0.252
fn+wn [1:4]	0.023	0.031	0.043	0.056	0.068	0.091	0.102	0.114	0.125	0.137	0.148
fn+wn [3:5]	0.048	0.058	0.075	0.090	0.105	0.132	0.145	0.157	0.170	0.182	0.194
fn+wn [5:3]	0.079	0.092	0.111	0.128	0.145	0.175	0.189	0.202	0.215	0.228	0.240
fn+wn [4:1]	0.089	0.102	0.120	0.137	0.152	0.181	0.194	0.206	0.219	0.230	0.242

Note. The offset parameters in the estimation represent evenly-spaced offsets within the time series.

Table A2
Velocity uncertainty inflation factors when parameters representing evenly-space offsets within a decade-long daily position time series are included in the estimation

	# of offset parameters											
Model	0	1	3	5	7	11	13	15	17	19	21	Sensitivity
white noise	1.000	2.019	3.988	5.982	7.976	11.964	13.957	15.951	17.945	19.939	21.933	0.996
fogm [0.8 days]	1.000	2.017	3.977	5.954	7.925	11.844	13.793	15.736	17.671	19.600	21.522	0.977
fogm [5 days]	1.000	1.941	3.581	5.055	6.384	8.724	9.771	10.755	11.683	12.566	13.403	0.585
fogm [10 days]	1.000	1.769	2.885	3.761	4.494	5.707	6.233	6.720	7.174	7.604	8.008	0.321
fogm [20 days]	1.000	1.453	1.984	2.387	2.726	3.294	3.542	3.774	3.991	4.196	4.391	0.152
fogm [50 days]	1.000	1.122	1.258	1.375	1.482	1.672	1.760	1.843	1.922	1.998	2.070	0.049
fogm [120 days]	1.000	1.025	1.055	1.082	1.109	1.160	1.185	1.209	1.233	1.256	1.279	0.013
fogm [180 days]	1.000	1.012	1.026	1.040	1.053	1.079	1.092	1.105	1.117	1.130	1.142	0.007
fogm [360 days]	1.000	1.003	1.008	1.012	1.017	1.025	1.029	1.033	1.038	1.042	1.046	0.002
fogm [600 days]	1.000	1.001	1.004	1.006	1.008	1.012	1.014	1.016	1.018	1.020	1.022	0.001
frac wn [-0.6]	1.000	1.439	2.119	2.729	3.289	4.314	4.792	5.254	5.700	6.134	6.556	0.260
frac wn [-0.8]	1.000	1.265	1.657	2.008	2.328	2.906	3.174	3.430	3.677	3.915	4.146	0.147
flicker I	1.000	1.129	1.319	1.493	1.654	1.949	2.086	2.218	2.345	2.467	2.586	0.074
flicker II	1.000	1.109	1.273	1.423	1.563	1.820	1.941	2.056	2.168	2.276	2.380	0.065
flicker III	1.000	1.141	1.363	1.567	1.753	2.096	2.254	2.405	2.551	2.692	2.828	0.086
frac rw [-1.4]	1.000	1.015	1.039	1.062	1.084	1.128	1.150	1.171	1.192	1.212	1.233	0.011
frac rw [-1.6]	1.000	1.004	1.010	1.017	1.023	1.036	1.042	1.048	1.055	1.061	1.067	0.003
random walk	1.000	1.000	1.000	1.001	1.001	1.002	1.002	1.002	1.002	1.003	1.003	0.000
fn+wn [1:4]	1.000	1.320	1.852	2.374	2.883	3.878	4.369	4.858	5.344	5.829	6.311	0.251
fn+wn [3:5]	1.000	1.220	1.561	1.881	2.182	2.748	3.017	3.281	3.538	3.791	4.040	0.143
fn+wn [5:3]	1.000	1.160	1.401	1.622	1.828	2.205	2.382	2.552	2.716	2.876	3.031	0.095
fn+wn [4:1]	1.000	1.137	1.342	1.529	1.701	2.018	2.166	2.307	2.444	2.576	2.704	0.080

Note. The inflation factor is defined as the ratio of the velocity uncertainty estimate with offsets to that without offsets. The sensitivity of velocity uncertainties to position offsets is measured by the fitted linear increasing rate of the inflation factor as the number of offsets increases.

Acknowledgments
This research is supported by NASA NIP Grant 80NSSC18K0748 and NASA ESI Grant 80NSSC18K0457. The PBO data analyzed for this study are available in the open archive located at UNAVCO (ftp://data-out.unavco.org/pub/products/position). We thank JGR Editor Paul Tregoning and three anonymous reviewers for the helpful suggestions.

References

Agnew, D. C. (1992). The time-domain behavior of power-law noises. *Geophysical Research Letters*, *19*(4), 333–336. https://doi.org/10.1029/91GL02832

Altamimi, Z., Sillard, P., & Boucher, C. (2002). ITRF2000: A new release of the international terrestrial reference frame for Earth science applications. *Journal of Geophysical Research*, *107*(B10), 2214. https://doi.org/10.1029/2001JB000561

Bock, Y., & Melgar, D. (2016). Physical applications of GPS geodesy: A review. *Reports on Progress in Physics*, *79*(10), 106,801.

Bos, M. S., Fernandes, R. M. S., Williams, S. D. P., & Bastos, L. (2013). Fast error analysis of continuous gnss observations with missing data. *Journal of Geodesy*, *87*(4), 351–360. https://doi.org/10.1007/s00190-012-0605-0

Floyd, M., & Herring, T. A. (2019). Geodetic time series analysis in earth sciences. In J.-P. Montillet, & M. Bos (Eds.), *Fast Statistical Approaches to Geodetic Time Series Analysis* (pp. 157–183). Switzerland: Springer Nature. https://doi.org/10.1007/978-3-030-21718-1

Gardner, M. (1978). White and brown music, fractal curves and one-over-f fluctuations. *Scientific American*, *238*(4), 16–27.

Gazeaux, J., Williams, S., King, M., Bos, M., Dach, R., Deo, M., et al. (2013). Detecting offsets in GPS time series: First results from the detection of offsets in GPS experiment. *Journal of Geophysical Research: Solid Earth*, *118*, 2397–2407. https://doi.org/10.1002/jgrb.50152

Golub, G., & Van Loan, C. (2013). Matrix computations. Johns Hopkins studies in the mathematical sciences: Johns Hopkins University Press.

Griffiths, J., & Ray, J. (2016). Impacts of GNSS position offsets on global frame stability. *Geophysical Journal International*, *204*(1), 480–487. https://doi.org/10.1093/gji/ggv455

Gross, R., Beutler, G., & Plag, H.-P. (2009). Integrated scientific and societal user requirements and functional specifications for the GGOS. In H.-P. Plag, & M. Pearlman (Eds.), *Global geodetic observing system: Meeting the requirements of a global society on a changing planet in 2020* (pp. 209–224). Berlin, Heidelberg: Springer Berlin Heidelberg.

Herring, T. A., Melbourne, T. I., Murray, M. H., Floyd, M. A., Szeliga, W. M., King, R. W., et al. (2016). Plate boundary observatory and related networks: GPS data analysis methods and geodetic products. *Reviews of Geophysics*, *54*, 759–808. https://doi.org/10.1002/2016RG000529

Hosking, J. R. M. (1981). Fractional differencing. *Biometrika*, *68*(1), 165–176.

Kasdin, N. J. (1995). Discrete simulation of colored noise and stochastic processes and $1/f^{\alpha}$ power law noise generation. *Proceedings of the IEEE*, *83*(5), 802–827. https://doi.org/10.1109/5.381848

Langbein, J., & Johnson, H. (1997). Correlated errors in geodetic time series: Implications for time-dependent deformation. *Journal of Geophysical Research*, *102*(B1), 591–603.

Mandelbrot, B. B., & Ness, J. W. V. (1968). Fractional Brownian motions, fractional noises and applications. *SIAM Review*, *10*(4), 422–437. https://doi.org/10.1137/1010093

Mao, A., Harrison, C. G. A., & Dixon, T. H. (1999). Noise in GPS coordinate time series. *Journal of Geophysical Research*, *104*(B2), 2797–2816. https://doi.org/10.1029/1998JB900033

Rebischung, P., Altamimi, Z., Ray, J., & Garayt, B. (2016). The IGS contribution to ITRF2014. *Journal of Geodesy*, *90*(7), 611–630. https://doi.org/10.1007/s00190-016-0897-6

Santamaría-Gómez, A., Bouin, M.-N., Collilieux, X., & Wöppelmann, G. (2011). Correlated errors in GPS position time series: Implications for velocity estimates. *Journal of Geophysical Research*, *116*, B01405. https://doi.org/10.1029/2010JB007701

Titchmarsh, E. C. (1968). *The theory of functions*, (2nd ed.). London: Oxford University Press.

Williams, S. D. P. (2003a). Offsets in Global Positioning System time series. *Journal of Geophysical Research*, *108*(B6), 2310. https://doi.org/10.1029/2002JB002156

Williams, S. D. P. (2003b). The effect of coloured noise on the uncertainties of rates estimated from geodetic time series. *Journal of Geodesy*, *76*(9-10), 483–494. https://doi.org/10.1007/s00190-002-0283-4

Williams, S. D. P., Bock, Y., Fang, P., Jamason, P., Nikolaidis, M. R., Prawirodirdjo, L., et al. (2004). Error analysis of continuous GPS position time series. *Journal of Geophysical Research*, *109*, B03412. https://doi.org/10.1029/2003JB002741

Wornell, G. W. (1993). Wavelet-based representations for the 1/f family of fractal processes. *Proceedings of the IEEE*, *81*(10), 1428–1450. https://doi.org/10.1109/5.241506

Zhang, J., Bock, Y., Johnson, H., Fang, P., Williams, S., Genrich, J., et al. (1997). Southern California permanent GPS geodetic array: Error analysis of daily position estimates and site velocities. *Journal of Geophysical Research*, *102*(B8), 18,035–18,055. https://doi.org/10.1029/97JB01380